Electronic structure and magnetic properties of small manganese oxide clusters

Myung Joon Han
School of Physics, Center for Strongly Correlated Materials Research, Seoul National University, Seoul 151-747, Korea

Taisuke Ozaki
Research Institute for Computational Sciences (RICS), National Institute of Advanced Industrial Science and Technology (AIST), 1-1-1 Umezono, Tsukuba, Ibaraki 305-8568, Japan

Jaejun Yu[a)]
School of Physics, Center for Strongly Correlated Materials Research, Seoul National University, Seoul 151-747, Korea

(Received 28 April 2005; accepted 23 May 2005; published online 28 July 2005)

To investigate the electronic structure and magnetic properties of manganese oxide clusters, we carried out first-principles electronic structure calculations for small MnO clusters. Among various structural and magnetic configurations of the clusters, the bulklike [111]-antiferromagnetic ordering is found to be favored energetically, while the surface atoms of the clusters exhibit interesting electronic and magnetic characteristics which are different from their bulk ones. The distinct features of the surface atoms are mainly attributed to the reduction of Mn coordination numbers and the bond-length contractions in the clusters, which may serve as a key factor for the understanding of physical and chemical properties of magnetic oxide nanoparticles. © *2005 American Institute of Physics*. [DOI: 10.1063/1.1953387]

I. INTRODUCTION

Recently physical and chemical properties of nanometer-sized particles have attracted a lot of attention due to their scientific and technological importance. The nanometer-sized materials often exhibit intriguing electrical, magnetic, optical, and chemical properties.[1–3] The magnetic nanoparticle is one of such subjects under intense investigations due to its potential application to ultrahigh-density storage devices[4] and catalysis.[5] There has been a great progress in the synthetic methodology and technique of magnetic oxide nanoparticles so that the size control, shape control, and mass production of transition-metal-oxide nanoparticles[6] can become possible.

Transition-metal-oxide clusters are expected to exhibit electronic, magnetic, and structural properties quite different from their "bulk" phase. Due to the presence of *d* electrons, the metal-oxide clusters often show unusual magnetic behaviors. Several experiments have reported a ferromagnetic behavior of nanosized MnO clusters contrary to its antiferromagnetic phase of the bulk MnO,[7–9] where the net magnetization was attributed to the spins at the surface of particles.[7,8] Moreover a recent measurement of the size-dependent magnetic properties strongly supports the idea of surface spins.[9] It was shown that MnO particles with the higher surface-to-volume ratio have the larger magnetic moment, implying that the ferromagnetism in MnO nanoparticles may originate from the surface spins.[9,10] Recently a density-functional study on $(MnO)_n$ clusters with $n \leqslant 9$ by Nayak and Jena[11,12] demonstrated that the small stoichiometric MnO clusters may be ferromagnetic with a sizable magnetic moment per MnO, which seems to be compatible to the observed ferromagnetic behavior of the MnO nanoparticles. However, it is still not certain how the experimental observation of the weak ferromagnetic signals is related to the magnetic ordering, that is, the origin of nanoscale ferromagnetism in the MnO clusters. To obtain a clear picture for the microscopic electronic structure and magnetic properties of MnO nanoparticles, we need to obtain more detailed information on the structure, size, and magnetic configurations of the clusters.

In this paper, to elucidate the relation between the cluster size and the magnetic configuration of MnO clusters, we present the results of our first-principles calculations on the $(MnO)_N$ clusters (N=6, 8, 9, 10, 12, and 15) with various spin configurations: ferromagnetic (FM) and [100]-, [010]-, [001]-, and [111]-antiferromagnetic (AFM) orders mimicking the bulk-phase orderings. From the total-energy results, it is found that the [111]-antiferromagnetic order, corresponding to the ordering of its bulk phase, still survives even in the small clusters, thereby the magnetic moments of the clusters are diminishing. While the [111] magnetic configuration is most stable energetically, the magnetic moments at the Mn site are found to depend on its coordination number.[7–9] We present the coordination-number dependence of the local electronic structure at Mn sites, where the contractions of the bond length are significant for the small size clusters and even a dangling-bond-like state appears at the corner Mn site with the threefold coordination.

[a)]Author to whom correspondence should be addressed. Electronic mail: jyu@snu-ac.kr

II. COMPUTATIONAL METHODS

We performed cluster calculations based on the density-functional theory (DFT) within the local spin-density approximation[13] (LSDA) by employing a linear combination of localized pseudoatomic orbitals (LCPAOs) method.[14] The generalized gradient approximation[15] (GGA) was also used for the purpose of confirming the results of LSDA. Double valence plus single polarization orbitals were used as a basis set, which are generated by a confinement potential scheme[14] with the cutoff radii of 7.0 a.u. for Mn and 5.0 a.u. for O. Troullier-Martins-type pseudopotentials[16] with a partial core correction[17] were used to replace the deep core potential by the norm-conserving soft potentials in a factorized separable form with the multiple projectors proposed by Blochl.[18] In the pseudopotential generation, the $3p$ states of Mn atoms were included as valence states in order to take account of the contribution of the semicore states to the electronic structures. Also the real-space grid techniques[19] were used with the energy cutoff up to 100 Ry in numerical integrations and the solution of the Poisson equation using the fast Fourier transformation (FFT) technique. All the DFT calculations were performed by using our code, OPENMX, which enables us to specify the initial spin configuration of individual atoms.[20]

III. RESULTS AND DISCUSSIONS

A. Equilibrium geometry and magnetic configuration

In search of the ground-state magnetic configuration of small MnO clusters, we consider rectilinearly stacked structures of the $(MnO)_N$ clusters (N=6, 8, 9, 10, 12, and 15), which resembles a fragment of the bulk MnO. Among the different stackings of (MnO) units, we determine the stable geometry of each $(MnO)_N$ cluster for a given number N. As illustrated in Fig. 1, it is found that there are two kinds of stable cluster structures: the "cubane-chain" structure for $(MnO)_N$ with N=6, 8, and 10 and the "stacked cubane-chain" structure for $(MnO)_N$ with N=9, 12, and 15. The Mn atoms in the former-type structures can be at most fourfold coordinated, while the latter can have up to fivefold-coordinated Mn atoms. Among the clusters which can form both the single cubane-chain and the stacked cubane-chain structures, we calculate the total energies of the two different stacked structures of $(MnO)_{12}$ clusters, for an example, and found that the $(MnO)_{12}$ cluster with the stacked cubane-chain structure is more stable by 0.829 eV in total energy for the same magnetic configuration. To determine the ground-state atomic structure of each cluster, we have carried out the total-energy calculations with full geometry optimization allowing the relaxation of all the atoms in the cluster. The geometry was optimized by the steepest descent (SD) method with a variable prefactor for accelerating the convergence until the maximum magnitude of the calculated force becomes below 10^{-3} Hartree/Bohr. In addition, to investigate the magnetic properties of the $(MnO)_N$ clusters, we probe several different spin configurations, which were imposed as an initial condition of the self-consistent calculation procedure. Possible spin configurations considered in this work include (i) FM and AFM configurations with (ii) [100], (iii) [010], (iv) [001], and (v) [111] orders, where [lmn] denotes the direction of the alternating FM layers with respect to the Cartesian axes of the stacked geometry as shown in Fig. 1. It is noted that the [111]-AFM ordered state is known to be the ground state of the bulk MnO. The [100], [010], and [001] configurations, although they were equivalent in the cubic MnO bulk phase, become inequivalent in a finite-size cluster.

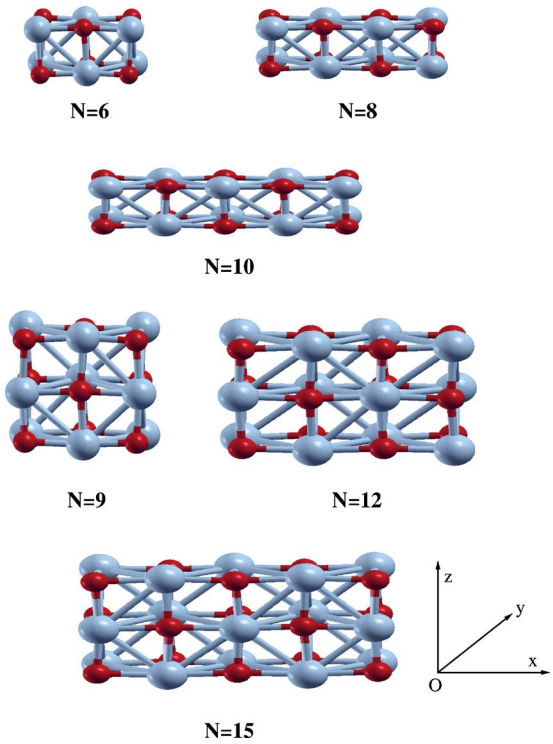

FIG. 1. (Color online) Structures of $(MnO)_N$ clusters calculated in this work. The dark (red) spheres represent Mn atoms and the bright (blue) ones O. The structure plots were generated by using the XCRYSDEN package (Ref. 24).

For each initial spin configuration, we obtained the fully relaxed structure and total energy of the $(MnO)_N$ cluster. Overall the structural properties of these clusters are quite different from the bulk ones. First, the equilibrium geometries of the clusters are significantly distorted from the bulk cubic structure, i.e., the angles between Mn and O atoms range from 85° to 95°. Second, the Mn–O bond lengths in the cluster $(MnO)_N$ (N=8–15) range from 1.9 to 2.0 Å, which corresponds to about 10% contraction compared to the bulk bond length of 2.22 Å. The bond-length contraction found for these small $(MnO)_N$ clusters seems to be consistent with previous studies on the structural relaxations of oxide surfaces and clusters.[21] The total energy per (MnO) unit in Fig. 2 shows a systematic variation as a function of the cluster size N, demonstrating that the larger the cluster size is, the more stable it becomes. For a given N, the total energy per (MnO) unit also depends on its magnetic configurations. Among them, the FM state has the highest energy in most cases, implying that the fully FM-polarized clusters can hardly exist. On the other hand, the [111]-AFM configuration is the most stable among all the clusters studied.

It is noted that our conclusion on the [111]-AFM configuration for the ground state of $(MnO)_N$ clusters is appar-

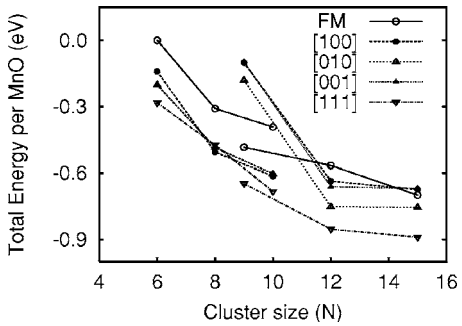

FIG. 2. The calculated ground-state enegies for each spin configuration as a function of the cluster size N. The total energy of $(MnO)_6$ with the FM configuration is used as a reference and the total energy is in unit of eV/(MnO) unit.

ently in contradiction to the prediction of the FM states for the small $(MnO)_N$ cluster ($N<8$) by Nayak and Jena in Refs. 11 and 12. Except for the different predictions on the magnetic ground state, however, most of the results on the bond lengths and total energies of the rectilinearly stacked structures of $(MnO)_N$ are in good agreement. Since the discrepancy in the magnetic ground state seems to be related to the use of different computational methods and the treatment of spin configurations, one needs to pursue the issue in future studies.

B. Coordination-number dependence of the local magnetic moment

While the [111]-AFM ordered configuration is stable energetically, the magnetic moment at each Mn site varies significantly from site to site. Taking the $N=12$ cluster as an example, there are three distinct Mn sites with different coordination numbers, i.e., $n=3-5$. Depending on the coordination number n, the magnitudes of the magnetic moment at Mn changes significantly. Figures 3(a)–3(c) show the ball-and-stick illustrations of the Mn–O bond lengths around the Mn atoms in the [111]-AFM $(MnO)_{12}$ cluster for the coordination numbers, $n=3-5$, respectively, while Fig. 3(d) shows the Mn atom in a bulk environment where the bond length between Mn and O is 2.22 Å. Our calculation result for the bulk case of Fig. 3(d) is in good agreement with the previous result in its bond length, i.e., $d=2.25$ Å (Refs. 11 and 12) as well as its magnetic moment.[22] In oxides, since the metal-ion-oxygen bonds have a mixed character of ionic and covalent bonding, the nature of structural relaxations around the atoms with low coordination numbers is rather subtle. Indeed it is suggested that the total energy of the metal-ion-oxygen bond should have strong contributions from all the components: short-range repulsion, Madelung potential, and covalent interactions.[21] Thus the competition between covalent and ionic interactions should play an important role in its structural distortions. The overall bond-length contractions by about 10% in our results are consistent with the previous works.[11,12] However, although the bond-length contraction of the rocksalt MgO is known to be larger around the atoms with a smaller coordination number,[21] our results for the $(MnO)_{12}$ cluster show a relatively small variation of the Mn–O bond lengths from $n=3-5$. It may be due to the small size of the clusters which we study here, where the effect of long-range Coulomb interactions, which is crucial in the bulk system, are absent due to its small size of the clusters. Therefore, a shorter Mn–O bond length in the case of a small cluster may play an important role in the change of electronic and magnetic structure at the surface, which will be discussed in Sec. III C.

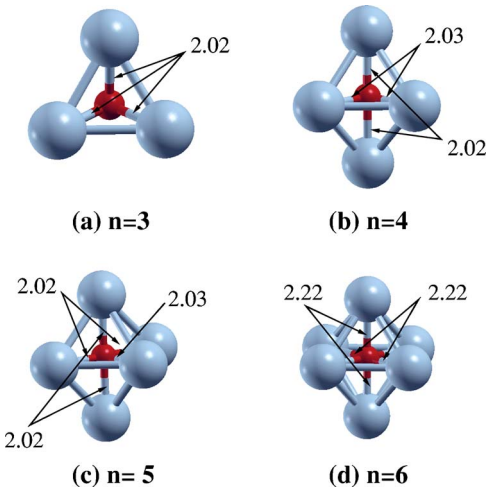

FIG. 3. (Color online) The coordination-number n dependence of bond lengths at selected Mn sites in $(MnO)_{12}$. The small dark (red) spheres represent the Mn atoms and the bright (blue) ones O. The bond lengths are in Å unit. The structure plots were generated by using the XCRYSDEN package (Ref. 24).

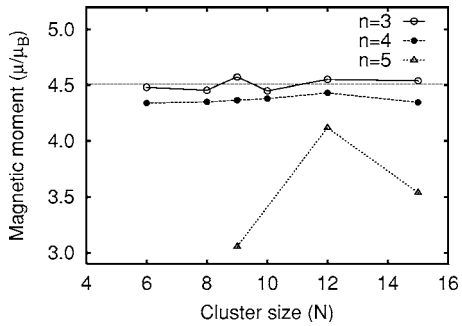

FIG. 4. The dependence of the Mn magnetic moment on the coordination number n.

It is interesting to note that the magnetic moment at the Mn site[23] depends on its coordination number n. One can clearly see that the Mn atom with a smaller coordination number n carries a larger magnetic moment. When $n=3$ and 4, Mn ion has the moments $\sim 4.5\mu_B$ and $4.4\mu_B$, respectively, which are comparable to the bulk magnetic moment of $4.51\mu_B$ (marked by a horizontal dotted line in Fig. 4). It is remarkable that the corner-Mn site ($n=3$) has a larger moment than the edge one ($n=4$) by about $0.1\mu_B$, while the magnetic moment at the $n=5$ site is notably smaller than others, $n=3$, 4, and 6. The general tendency of the magnetic-moment dependence on the coordination number may be understood by the change of the local electronic and magnetic structure.

C. Site-dependent electronic and magnetic structure

The bulk electronic and magnetic structure of the cubic MnO is well known. The formal valence of Mn ions in MnO

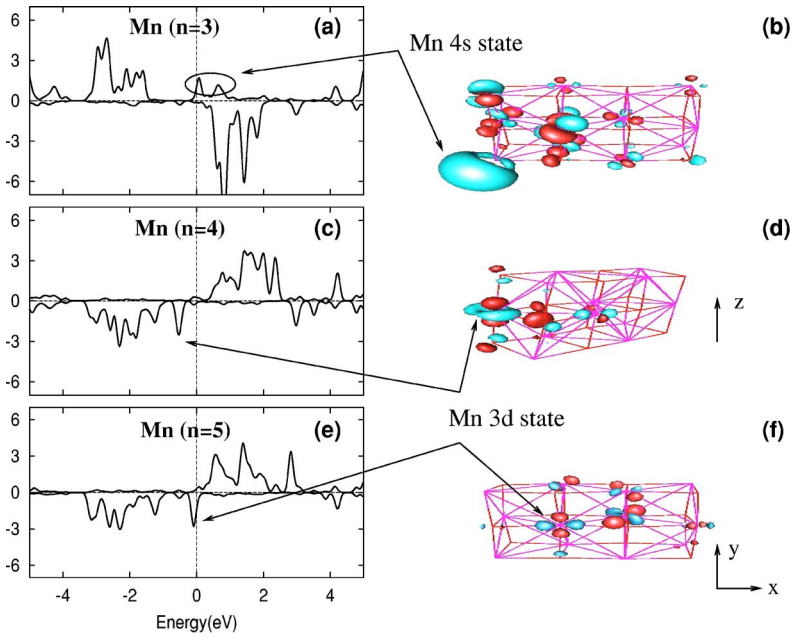

FIG. 5. (Color online) Projected density of states (pDOS) and the electronic states near the Fermi level at the Mn sites with the coordination number $n=3$ in (a) and (b), $n=4$ in (c) and (d), and $n=5$ in (e) and (f), respectively. In the three-dimensional (3D) contour plots (b), (d), and (f) of the electronic states, the dark (red) and bright (blue) colors represent the positive and negative phases of the wave function, respectively.

is 2+ so that the Mn ion has a high-spin d^5 configuration. Due to the large exchange splitting, in spite of the shortcomings of LSDA in the description of the correlated transition-metal-oxide systems, the DFT calculations with LSDA predicts at least a correct ground state with a reasonable magnetic moment and spin configuration for MnO. Contrary to the bulk electronic structure, there is no attempt so far to provide a detailed picture of the Mn electronic structure in $(MnO)_N$ clusters, which is crucial in understanding the physical and chemical properties of MnO nanoparticles.

Figure 5 shows the projected density of states (pDOS) and the corresponding electronic states near the Fermi level at the Mn sites of the $(MnO)_{12}$ cluster with the coordination number $n=3-5$, respectively. Depending on the local environment, i.e., the number of neighboring oxygen at each Mn site, the distributions of the Mn d states are quite different from each other. Not only the width of the Mn d levels but also the orbital characters near the Fermi level change significantly. For the Mn atom at the corner site, i.e., having only three neighboring oxygen ($n=3$) as shown in Figs. 5(a) and 5(b), the large exchange splitting in Mn-3d states gives rise to the magnetic moment of $4.55\mu_B$, which is larger than those of $n=4$ and 5. It is interesting to note that the Mn-4s state forms a dangling-bond-like state located near the Fermi level. The presence of the low-lying 4s state is attributed to the small coordination number of oxygen ions; due to the small number of negatively charged ions, the Coulomb repulsion energy for the 4s orbital becomes considerably reduced, which results in a dangling-bond Mn-4s state pinned at the Fermi level. This explanation is consistent with the contour plot of the corresponding wave function in Fig. 5(b), demonstrating a large s-type lobe protruding toward the vacuum region. Consequently, the Mn-4s dangling-bond state at the corner site of the cluster is expected to become an active site participating in chemical bonding.

When $n=4$, as shown in Figs. 5(c) and 5(d), all of the spin-down 3d states stay below the Fermi level just as when $n=3$. Thus its magnetic moment $m=4.43\mu_B$ becomes comparable to that of $n=3$. Regarding the width of Mn-3d states, it is obvious from the comparison of Figs. 5(a) and 5(c) that the 3d width of $n=4$ is much broader than that of $n=3$, which is due to the increase of the coordination number and the Mn–O hybridization. The slight decrease of the local moment at the Mn site from $m=4.55\mu_B$ ($n=3$) to $m=4.43\mu_B$ may be attributed to the increase of the Mn $d-$O p hybridization as well. Contrary to the presence of the Mn-4s dangling-bond state at the Fermi level for the $n=3$ case, the $n=4$ Mn site has a $(z^2-r^2/3)$-type 3d orbital state

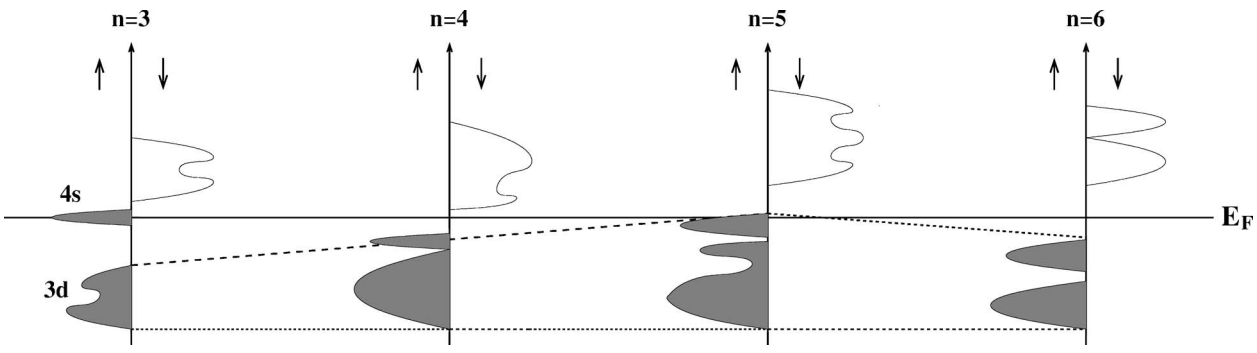

FIG. 6. Schematic energy diagram illustrating the change of the Mn electronic structure as a function of coordination number.

just below the Fermi level while the states with the Mn-4*s* character are pushed up by about 2 eV above the Fermi level.

As discussed in Sec. III B, the magnetic moment for $n=5$ is notably smaller compared to the other cases ($n=3$, 4, and 6). One possible reason for the reduction is the shift of the 3*d* orbitals toward the Fermi level, as shown in Fig. 5(e). Due to the absence of an oxygen neighbor in the *z* direction and the short bond length, one of the Mn-3*d* state with (x^2-y^2) character is located near the Fermi level, and the partially filled 3*d* orbital state contributes to the smaller magnetic moment.

In Fig. 6, we draw a schematic energy diagram illustrating the evolution of the local electronic structure at the Mn sites with the change of the coordination numbers. From $n=3$ to $n=5$, the width of the Mn 3*d* levels gets broader as *n* increases due to the Mn *d*–O *p* hybridization with increasing O neighbors. When $n=6$, i.e., the bulk environment, the width becomes reduced and the e_g and t_{2g} separated pDOS features are recovered. The reduction of the width is due to the longer bond length than those of the clusters. It is remarkable that for the case of $n=3$ the crystal-field splittings of the Mn 3*d* states are rather weak so the 3*d* pDOS width is relatively small. Further the dangling-bond-like Mn-4*s* state is pinned at the Fermi level. For $n=5$, the (x^2-y^2)-type 3*d* level is at the Fermi level due to the short bond length of the cluster, resulting in the large Jahn–Teller-type splitting, and the pyramidal structure with only one negatively charged ion in the *z* direction.

IV. CONCLUSION

In summary, we have performed first-principles calculations for the $(MnO)_N$ ($N=6-15$) clusters with various magnetic configurations. The calculated total energies show that the bulklike [111]-AFM configuration is energetically most stable, implying that fully ordered FM clusters can hardly exist. The calculated magnetic moments as a function of coordination numbers strongly suggest the surface spin moment can be enhanced significantly. From the electronic structure analysis we show that the surface magnetic structure in nanoclusters can be quite different from the bulk one mainly due to the reduction of the coordination numbers and the bond-length contractions. As the coordination number *n* decreases from $n=5$ to $n=3$, the bandwidth of the Mn-3*d* level becomes smaller, whereas the Mn magnetic moment becomes enhanced. Our results are expected to provide a basic framework of understanding the magnetic oxide nanoparticle in which the surface property rather than the bulk one is dominant.

ACKNOWLEDGMENTS

We are grateful to Professor T. Hyeon and Professor J.-G. Park for helpful discussions. This work was supported by the KOSEF through CSCMR and by the MOST through the NSTP (Grant No. M1-0213-04-0001). One of the authors (T.O.) was partially supported by NEDO under the Nanotechnology Materials Program, CREST under the Japan Science and Technology Agency, and NAREGI Nanoscience Project, Ministry of Education, Culture, Sports, Science and Technology, Japan.

[1] S. A. Majetich and Y. Jin, Science **284**, 470 (1999).
[2] C. B. Murray, C. R. Kagan, and M. G. Bawendi, Science **270**, 1335 (1995).
[3] A. J. Zarur and J. Y. Ying, Nature (London) **403**, 65 (2000).
[4] S. Sun, C. B. Murray, D. Weller, L. Folks, and A. Moser, Science **287**, 1989 (2000); D. D. Awschalom and D. P. DiVincenzo, Phys. Today **48**(4), 43 (1995); K. Raj and R. Moskowitz, J. Magn. Magn. Mater. **85**, 233 (1990); I. M. L. Billas, A. Chatelain, and W. A. de Heer, Science **265**, 1682 (1994).
[5] S.-W. Kim, M. Kim, W. Y. Lee, and T. Hyeon, J. Am. Chem. Soc. **124**, 7642 (2002); S.-W. Kim, S. U. Son, S. S. Lee, T. Hyeon, and Y. K. Chung, Chem. Commun. (Cambridge) **2001**, 2212 (2001).
[6] T. Hyeon, Chem. Commun. (Cambridge) **2003**, 927, and references therein.
[7] J. Li, Y. J. Wang, B. S. Zou, X. C. Wu, J. G. Lin, L. Guo, and Q. S. Li, Appl. Phys. Lett. **70**, 3047 (1997).
[8] G. H. Lee, S. H. Huh, J. W. Jeong, B. J. Choi, S. H. Kim, and H.-C. Ri, J. Am. Chem. Soc. **124**, 12094 (2002).
[9] W. S. Seo, H. H. Jo, K. Lee, B. Kim, S. J. Oh, and J. T. Park, Angew. Chem., Int. Ed. **43**, 1115 (2004).
[10] J. Park, E. Kang, C. J. Bae, J.-G. Park, H.-J. Noh, J.-Y. Kim, J.-H. Park, H. M. Park, and T. Hyeon, J. Phys. Chem. B **108**, 13594 (2004).
[11] S. K. Nayak and P. Jena, Phys. Rev. Lett. **81**, 2970 (1998).
[12] S. K. Nayak and P. Jena, J. Am. Chem. Soc. **121**, 644 (1999).
[13] D. M. Ceperley and B. J. Alder, Phys. Rev. Lett. **45**, 566 (1980); J. P. Perdew and A. Zunger, Phys. Rev. B **23**, 5048 (1981).
[14] T. Ozaki, Phys. Rev. B **67**, 155108 (2003); T. Ozaki and H. Kino, *ibid.* **69**, 195113 (2004); T. Ozaki and H. Kino, Phys. Rev. B (to be published).
[15] J. P. Perdew, K. Burke, and M. Ernzerhof, Phys. Rev. Lett. **77**, 3865 (1996).
[16] N. Troullier and J. L. Martins, Phys. Rev. B **43**, 1993 (1991).
[17] S. G. Louie, S. Froyen, and M. L. Cohen, Phys. Rev. B **26**, 1738 (1982).
[18] P. E. Blochl, Phys. Rev. B **41**, 5414 (1990).
[19] J. Junquera, O. Paz, D. Sanchez-Portal, and E. Artacho, Phys. Rev. B **64**, 235111 (2001); J. M. Soler, E. Artacho, J. D. Gale, A. Garcia, J. Junquera, P. Ordejon, and D. Sanchez-Portal, J. Phys.: Condens. Matter **14**, 2745 (2002), and references therein.
[20] Our DFT code, OPENMX, the primitive orbitals, and pseudopotentials ranging from H to Kr used in this study are available on a web site (http://staff. aist.go.jp/t-ozaki/) in the constitution of the GNU General Public Licence.
[21] C. Noguera, *Physics and Chemistry at Oxide Surfaces* (Cambridge University press, Cambridge, 1996), and references therein.
[22] A. K. Cheetham and D. A. O. Hope, Phys. Rev. B **27**, 6964 (1983); V. I. Anisimov, J. Zaanen, and O. K. Andersen, *ibid.* **44**, 943 (1991); M. Arai and T. Fujiwara, *ibid.* **51**, 1477 (1995).
[23] R. S. Mulliken, J. Chem. Phys. **23**, 1833 (1955).
[24] A. Kokalj, J. Mol. Graphics Modell. **17**, 176 (1999); http://www.xcrysden.org/